Shell model and octupole excitations in ^{147}Eu

Zs. Podolyák,[1,2] P. G. Bizzeti,[3] A. M. Bizzeti-Sona,[3] A. Gadea,[2,5] S. Lunardi,[4] D. Bazzacco,[4] G. de Angelis,[2] M. De Poli,[2] D. R. Napoli,[2] C. M. Petrache,[4,*] C. Rossi Alvarez,[4] C. A. Ur,[4,†] P. Kleinheinz,[5,6] and J. Blomqvist[7]

[1]*Department of Physics, University of Surrey, Guildford GU2 7XH, United Kingdom*

[2]*INFN, Laboratori Nazionali di Legnaro, Legnaro, Italy*

[3]*Dipartimento di Fisica dell'Università and INFN, Sezione di Firenze, Firenze, Italy*

[4]*Dipartimento di Fisica dell'Università and INFN, Sezione di Padova, Padova, Italy*

[5]*Instituto de Física Corpuscular, Valencia, Spain*

[6]*Institut für Kernphysik, Forschungszentrum Jülich, Jülich, Germany*

[7]*Department of Physics Frescati, Royal Institute of Technology, Stockholm, Sweden*

(Received 15 March 2001; published 27 July 2001)

The structure of the ^{147}Eu nucleus has been studied via the ^{124}Sn(^{28}Si,$p4n$) fusion-evaporation reaction at 125 MeV beam energy. The yrast level scheme has been extended up to 10 MeV and spin near 55/2. Up to the highest spins the levels are interpreted in terms of specific multinucleon excitations involving up to seven quasiparticles. Parameter free shell model calculations for three or five nucleons, or for three nucleons and an octupole phonon, are in good agreement with experiment for all the states observed here below 4.2 MeV, and also with the above-yrast levels known from earlier (p,$2n$) experiments.

DOI: 10.1103/PhysRevC.64.034302 PACS number(s): 23.20.Lv, 25.70.Gh, 27.60.+j

I. INTRODUCTION

The $^{147}_{63}$Eu$_{84}$ nucleus has two valence neutrons and a proton hole with respect to the doubly closed ^{146}Gd core nucleus. Therefore, it is expected that the low spin yrast structure is dominated by shell model excitations, with the two valence neutrons and the odd proton occupying the available single-particle orbitals near the Fermi surface. At higher spin and excitation energy, levels arising from the coupling of the valence particles with the states of the ^{146}Gd core should become energetically favored, with its 3^- first excited state playing a major role. In fact, it is well established from the study of nuclei around ^{146}Gd that the addition of valence neutrons significantly lowers the 3^- energy [1,2]. We therefore expect that octupole vibrations play an important role in ^{147}Eu also.

In ^{147}Eu the two valence neutrons can occupy the shell model orbitals above $N=82$, where the $2f_{7/2}$, $1h_{9/2}$, and $1i_{13/2}$ orbitals are most effective for building up high spin states. High spin orbitals available to the odd proton are $2d_{5/2}$ and $1g_{7/2}$ below $Z=64$ and $1h_{11/2}$ above, and in fact the $\pi d_{5/2}^{-1}$, $\pi g_{7/2}^{-1}$, and $\pi h_{11/2}$ single-proton orbitals form the lowest three states of ^{147}Eu at 0, 230, and 625 keV, where the last is an $M2+E3$ isomer [3] with a half-life of 0.77 μs. In a heavy ion experiment, like the one presented in this article, we expect to populate predominantly the levels with the odd proton in the $h_{11/2}$ orbital.

Early studies of ^{147}Eu from ^{147}Gd($7/2^-$) β decay [4] provided knowledge of low spin excitations up to 2.2 MeV, and (t,α) transfer experiments with a radioactive ^{148}Gd target [5] gave results on the single-proton-hole strengths. An early (p,$2n\gamma$) experiment [6] together with a later similar study including conversion electron measurements also [7] located the yrast states up to $(23/2)^-$ at 2.3 MeV and many above-yrast levels with spins up to $(21/2)^-$.

The ^{147}Eu high spin structure was studied in (^{7}Li,$3n\gamma$) and (^{12}C,$4n\gamma$) reactions by Fleissner *et al.* [8], who interpreted the observed levels as favored and unfavored members of a decoupled band built on the $11/2^-$ state, and as the $h_{11/2}$ couplings to the ^{146}Sm7^-, 8^+, and 9^- core yrast states. More recently, in a parallel study with the (^{13}C,$5n\gamma$) reaction, Zhou *et al.* [9] identified many new ^{147}Eu high spin states up to 8 MeV, with spins assigned up to 41/2 at 5.8 MeV. The authors compared the ^{147}Eu level energies with the yrast energies of ^{148}Gd added to the ^{145}Eu $\pi d_{5/2}^{-1}$ and $\pi g_{7/2}^{-1}$ states, or of ^{146}Sm added to the $\pi h_{11/2}$ energy, but without assigning specific configurations to individual ^{147}Eu levels.

The ^{147}Eu nucleus has also been studied at Gammasphere in order to extend the knowledge of nuclear superdeformation in the $A=150$ mass region. Indeed, six superdeformed bands have been identified from their coincidence with the three lowest yrast transitions above the $\pi h_{11/2}$ isomer [10].

We report in this article a detailed study of ^{147}Eu, with the goal of elucidating its high spin structure. The observed states are discussed in terms of multiparticle and octupole excitations around the ^{146}Gd core based on parameter free shell model calculations.

II. MEASUREMENTS AND RESULTS

The ^{147}Eu nucleus was populated through the ^{124}Sn(^{28}Si,$p4n$) reaction at a beam energy of 125 MeV. The beam was delivered by the Tandem XTU accelerator of Legnaro National Laboratories. A 97% isotopically enriched 3.4 mg/cm^2 thick ^{124}Sn target on a 15.5 mg/cm^2 >99% enriched ^{208}Pb backing was used.

The GASP array [11] in configuration II, with 40 Comp-

*Permanent address: Dipartimento di Fisica dell'Università di Camerino, Camerino, Italy.

†Permanent address: Institute of Physics and Nuclear Engineering, Bucharest, Romania.

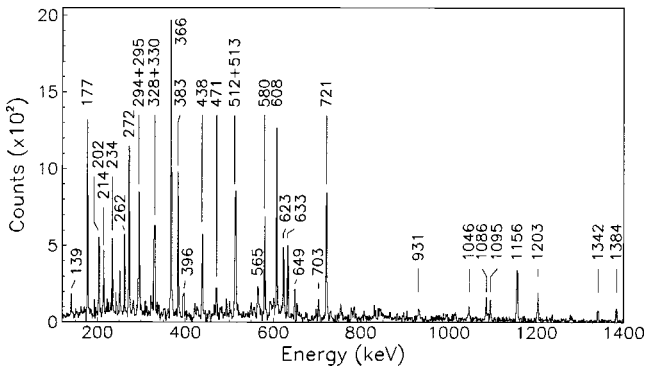

FIG. 1. Doubly gated coincidence spectrum with the first gate on the 562 keV ($43/2^+ \rightarrow 41/2^+$) transition and with the second gate on the 580 keV ($19/2^- \rightarrow 15/2^-$) or on the 721 keV ($15/2^- \rightarrow 11/2^-$) transition.

ton suppressed HPGe detectors of 70–90 % relative efficiency, was used for γ-ray detection. In this configuration the average distance between target and Ge detectors is reduced to about 20 cm by removing the multiplicity filter, thereby achieving 5.8% photopeak efficiency at 1.3 MeV, twice more than in the standard configuration. The requirement for collecting events was a minimum of three coincident signals from suppressed Ge detectors.

Energy calibration of the spectra and gain matching of the Ge detectors was performed using standard γ-ray sources as well as known γ-ray transitions from the main reaction products. The errors of the transition energies extracted are at most 0.3 keV.

The data were sorted into symmetrized $\gamma\gamma$ matrices and $\gamma\gamma\gamma$ cubes. An example showing a doubly gated spectrum in ^{147}Eu from the data is given in Fig. 1.

Multipolarities for the ^{147}Eu transitions were deduced from analysis of the directional correlation ratios of oriented states (DCO). A DCO $\gamma\gamma$ matrix was created by sorting on one axis the detectors lying at 90° with respect to the beam direction and on the other axis the detectors at 34° and 146°. In the GASP geometry, with a gate on a stretched quadrupole transition, the theoretical DCO ratio $I_{34°}$ (gated at 90°)/$I_{90°}$ (gated at 34°) is 1.0 for stretched quadrupole transitions and 0.5 for stretched pure dipoles. With the gate on a dipole transition, the expected ratios for quadrupole and dipole transitions are 2.0 and 1.0, respectively. In our analysis we used gates on stretched quadrupole transitions. The DCO values for low energy transitions have large uncertainties due to the absorption in the target frame, which strongly reduces their detection at 90°.

The energies, intensities, and DCO ratios of the γ transitions of ^{147}Eu, together with their placements in the level scheme and the adopted spin-parity assignments, are compiled in Table I. The intensities are normalized to the 580.2 keV $19/2^- \rightarrow 15/2^-$ transition, which specifies the intensity of the $p4n$ exit channel. In our experiment we clearly observe all ^{147}Eu γ rays down to 1% of this intensity.

III. THE LEVEL SCHEME OF ^{147}Eu

The level scheme of the ^{147}Eu nucleus deduced from the present study is shown in Fig. 2. The observed levels are arranged in the figure in separate columns corresponding to their assigned nuclear structure. The transitions have been placed on the basis of coincidence relationships and intensities.

Spin assignments are derived from the adopted transition multipolarities specified in Table I, and from decay patterns. The parity of the levels is more difficult to establish, having at disposal DCO ratios only. In our experiment only the transitions with ratios definitively different from 0.5 and 1.0 can give firm parity information. These transitions are presumed to be of mixed $M1+E2$ character and therefore connect levels with the same parity. Table I includes two such examples, $E_\gamma = 512$ and 562 keV. There exists, however, no clear-cut DCO result that firmly identifies parity-changing radiation. A DCO value of unity is usually taken as indicative of a stretched $E2$ transition, but it can, for example, equally well be $\Delta I = 0$ dipole radiation. In fact, $\Delta I = 0 E1$ as well as $M1$ transitions are not rare in this nuclear region (cf., e.g., ^{148}Gd [1] or ^{149}Tb [2], and also ^{147}Eu).

In view of these difficulties it becomes necessary to resort to other information for parity assignment. This could be, e.g., shell model calculations, which, however, should provide unique correspondence with the observed states and thus can specify their parities. We will present such calculations in Sec. V. Moreover, in our case we also gain crucial parity information from comparison with the isotone ^{149}Tb. This nucleus was recently investigated in (α,6n) and (^{7}Li,2n) in-beam experiments, including γ-ray angular distribution and polarization measurements [2], which provided the ^{149}Tb high spin states up to $41/2^{(+)}$ at 5.1 MeV, with level parities firmly established for almost all states. Subsequent conversion electron measurements in a (^{31}P,4n) experiment [12] have independently confirmed these results.

An astounding similarity of the two $N=84$ isotones is apparent for the high spin states up to 5 MeV above the respective $11/2^-$ isomers in the two nuclei (see Fig. 3). Thirteen of the 14 levels observed here in ^{147}Eu below 4.25 MeV have counterparts in ^{149}Tb, at very similar excitation above the $11/2^-$ state, and with essentially the same γ decay patterns. In the 1.5 MeV interval above, from $33/2^+$ to $41/2^+$, our data have identified many more states in ^{147}Eu than are known in ^{149}Tb, but they also clearly single out seven ^{147}Eu levels as the counterparts of the seven highest states observed in ^{149}Tb [2] in the corresponding energy region. In all cases our spins measured for the states agree with those of their partners in ^{149}Tb, and their excitation energies above the $11/2^-$ level agree on the average within 50 keV; the largest observed deviation is 122 keV. In view of this astonishing quantitative correspondence we conclude that the structural nature of the levels and therewith also their parities almost certainly must be the same in the two nuclei.

Above $41/2^+$ at 5772 keV we firmly assign $43/2^+$ to the next level from the the $M1+E2$ character of the 562 keV γ ray, but for all levels above there are no conclusive data to specify the parities. Also the comparison with ^{149}Tb, where spins and parities were measured up to $75/2^{(-)}$ [12], does not provide elucidation since above $41/2^+$ there is a complete lack of any correspondence between the levels of the two

TABLE I. Energies, intensities, DCO ratios, and placement of γ transitions assigned to ^{147}Eu from the ^{124}Sn+^{28}Si reaction at 125 MeV.

E_γ (keV)[a]	I_γ (%)[b]	DCO[c]	$J_i^\pi \rightarrow J_f^\pi$	E_i (keV)
40[d]	2.4[e]		$27/2^+ \rightarrow 25/2^-$	3230
54[d]	1.8[e]		$21/2^- \rightarrow 23/2^-$	2347
119	~1		$45/2^{(-)} \rightarrow 45/2$	6966
134.3	1.6(9)	0.61(32) D	$45/2 \rightarrow 43/2$	6847
139.3	3.4(19)	0.66(32) (D)	$39/2^+ \rightarrow 37/2$	5595
162.4	1.5(8)		$39/2^+ \rightarrow$	5595
164.0	0.9(7)		$53/2^{(-)} \rightarrow 51/2^{(-)}$	8776
176.8	18.0(25)	0.51(8) D	$41/2^+ \rightarrow 39/2^+$	5772
183.4	2.9(11)	0.63(18) D	$45/2 \rightarrow 43/2$	6847
201.7	3.3(17)	0.48(17) D	$37/2^+ \rightarrow 35/2$	5083
202.3	6.3(13)	0.46(14) D	$47/2^{(-)} \rightarrow 45/2^{(-)}$	7168[f]
213.7	8.3(7)	0.56(15) D	$39/2^+ \rightarrow 37/2^+$	5595
221.7	1.5(9)		$39/2^+ \rightarrow 35/2,39/2$	5595
229.7	75[e]	$M1$[e]	$7/2^+ \rightarrow 5/2^+$	230
233.7	16.1(16)	0.84(15) Q	$27/2^+ \rightarrow 23/2^+$	3230
241.9	3.5(6)	0.39(15) D	$35/2 \rightarrow 33/2^{(-)}$	4881[g]
250.3	6.0(12)	0.57(13) D	$35/2 \rightarrow 33/2^+$	4862
261.7	12.6(9)	0.66(14) D	$39/2^+ \rightarrow 37/2^+$	5595
268.8	2.6(6)	0.86(21) D[h], Q	$35/2,39/2 \rightarrow 35/2$	5176[i]
271.7	33.1(23)	0.54(7) D	$31/2^+ \rightarrow 29/2^+$	3795
281.4	2.0(6)		$37/2^+ \rightarrow 33/2^+$	5083
290.3	2.5(7)	0.46(15) D	$25/2^- \rightarrow 27/2^-$	3190
293.7	26(3)	0.50(6) D	$29/2^+ \rightarrow 27/2^+$	3523
295.4	8.8(8)	0.45(8) D	$35/2 \rightarrow 33/2^+$	4907
312.4	1.4(8)		$\rightarrow 35/2,39/2$	5685[g]
324.3	2.4(10)	0.52(13) D	$37/2^+ \rightarrow 35/2^+$	5381
328.1	11.1(19)	0.54(7) D	$33/2^+ \rightarrow 31/2^-$	4612
329.6	17.8(21)	0.96(12) D[h]	$27/2^+ \rightarrow 27/2^-$	3230
337.4	2.8(8)	0.55(13) D	$45/2 \rightarrow 43/2$	6847
339.0	1.1(6)			6024[i]
345.6	1.4(7)		$25/2^- \rightarrow 23/2^-$	3190
366.4	94(5)	0.97(6) Q	$23/2^- \rightarrow 19/2^-$	2293
369.7	6.0(9)	0.51(6) D	$33/2^+ \rightarrow 31/2^-$	4612
382.9	27.3(24)	0.43(5) D	$33/2^+ \rightarrow 31/2^+$	4178
395.7	77[e]	$M2$[e]	$11/2^- \rightarrow 7/2^+$	625
420.9	4.4(4)	0.42(8) D	$21/2^- \rightarrow 19/2^-$	2347
426.6	2.8(5)	0.43(11) D	$37/2^+ \rightarrow 35/2$	5333
438.1	7.5(7)	0.95(11) Q	$41/2^+ \rightarrow 37/2^+$	5772
447.7	1.2(3)	0.83(20) D[h]	$31/2^- \rightarrow 31/2^+$	4242
456.1	2.2(9)	0.41(20) D	$45/2^{(-)} \rightarrow 43/2$	6966
465.5	3.1(4)	0.83(16) D[h], Q	$35/2,39/2 \rightarrow 35/2$	5373
470.5	4.3(5)	0.87(16) Q	$37/2^+ \rightarrow 33/2^+$	5083
491.8	1.4(5)		$23/2^+ \rightarrow 19/2^+$	2996
492.2	2.0(9)		$\rightarrow 53/2^{(-)}$	9269
497.5	1.7(8)	0.39(19) D	$23/2^- \rightarrow 21/2^-$	2845[f]
499.4	2.1(9)	0.69(25) (D)	$(35/2) \rightarrow 33/2^+$	4677
512.3	10.4(27)	0.74(8) $D+Q$	$39/2^+ \rightarrow 37/2^+$	5595
513.3	6.2(13)	0.53(9) D	$49/2^{(-)} \rightarrow 47/2^{(-)}$	7682
548.4	3.4(5)	0.60(11) D	$37/2 \rightarrow 35/2$	5456
561.8	12.8(14)	0.72(8) $D+Q$	$43/2^+ \rightarrow 41/2^+$	6333
565.1	8.5(9)	1.02(12) Q	$31/2^+ \rightarrow 27/2^+$	3795
578.0	1.1(9)		$19/2^+ \rightarrow 19/2^-$	2504[f]
580.2	100	0.97(6) Q	$19/2^- \rightarrow 15/2^-$	1927
593.5	2.2(13)	0.66(21) D	$37/2 \rightarrow 35/2$	5456
607.5	66(4)	1.02(7) Q	$27/2^- \rightarrow 23/2^-$	2900
622.8	21.5(17)	0.47(5) D	$29/2^+ \rightarrow 27/2^-$	3523
625.3	10[e]	$E3$[e]	$11/2^- \rightarrow 5/2^+$	625
632.8	3.3(6)	0.54(10) D	$45/2^{(-)} \rightarrow 43/2^+$	6966
648.7	9.4(8)	0.51(6) D	$23/2^+ \rightarrow 21/2^-$	2996
654.4	3.7(5)	0.93(19) Q	$33/2^+ \rightarrow 29/2^+$	4178
657	1.4(6)		$37/2^+ \rightarrow (35/2)$	5333
703.3	8.8(6)	0.84(12) D[h]	$23/2^+ \rightarrow 23/2^-$	2996
721.0	100[e]	$E2$[e]	$15/2^- \rightarrow 11/2^-$	1346
730.2	1.3(6)	0.32(16) D	$35/2 \rightarrow 33/2^+$	4907
738.3	7.0(6)	0.47(8) D	$43/2 \rightarrow 41/2^+$	6510
754.0	1.5(9)		$\rightarrow (35/2)$	5432[f]
757	0.7(5)			9269
830.3	1.6(8)		$\rightarrow 49/2^{(-)}$	8512[g]
844.6	3.3(11)		$33/2^{(-)} \rightarrow 31/2^+$	4639[g]
866.5	1.3(6)		$\rightarrow 53/2^{(-)}$	9643[i]
892.3	3.2(5)	0.52(13) D	$43/2 \rightarrow 41/2^+$	6664[g]
931.4	2.3(8)	0.57(13) D	$51/2^{(-)} \rightarrow 49/2^{(-)}$	8612[g]
941.5	3.4(5)	0.42(12) D	$43/2 \rightarrow 41/2^+$	6713
1045.5	2.7(12)		$\rightarrow 49/2^{(-)}$	8728[i]
1086.2	1.6(9)		$\rightarrow 43/2^+$	7420[i]
1094.7	3.5(16)	1.19(23) Q	$53/2^{(-)} \rightarrow 49/2^{(-)}$	8776
1155.6	15.9(12)	0.94(9) Q	$37/2^+ \rightarrow 33/2^+$	5333
1191.2	2.9(5)	0.84(27) (Q)	$45/2^+ \rightarrow 41/2^+$	6963[i]
1203.2	7.6(6)	0.86(16) Q	$37/2^+ \rightarrow 33/2^+$	5381
1261.4	2.5(9)	1.29(35) Q	$35/2^+ \rightarrow 31/2^+$	5056[f]
1277.9	2.5(4)	1.14(31) Q	$33/2^+ \rightarrow 29/2^+$	4801[f]
1341.8	6.3(5)	0.99(15) Q	$31/2^- \rightarrow 27/2^-$	4242
1383.5	11.2(9)	0.86(14) Q	$31/2^- \rightarrow 27/2^-$	4284[f]

[a]Energy error $\leqslant$0.3 keV.

[b]In percent of the $p4n$ exit channel cross section. Extracted from coincidence data, largely with gate on 721 keV $15/2^- \rightarrow 11/2^-$.

[c]Listed is the intensity ratio $I_{34°}$ (gated at 90°)/$I_{90°}$ (gated at 34°) with gate on the $15/2^-$ to $11/2^-$ stretched $E2$ transition, together with the adopted stretched quadrupole or dipole multipolarity.

[d]Unobserved transition firmly established from coincidence results.

[e]Implied from level scheme or Ref. [3].

[f]Energy ambiguous from intensity data, but preferred from theory or from decay branchings of the feeding state.

[g]Ambiguous level energy.

[h]Adopted as $\Delta I = 0$ dipole radiation.

[i]Monopode.

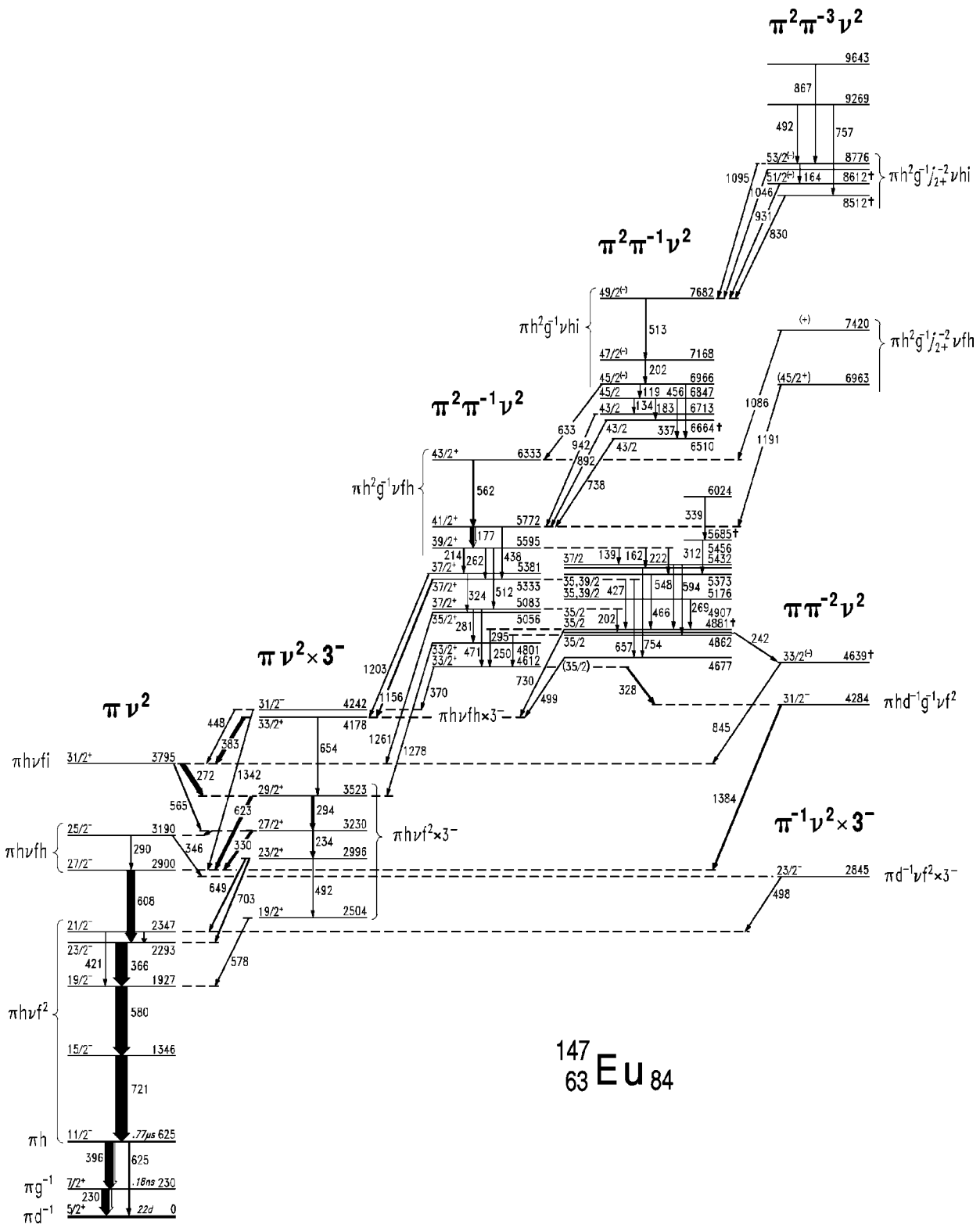

FIG. 2. Level scheme of ^{147}Eu as observed in the present experiment. The energy levels are arranged in separate columns according to their structural complexity specified above by the number of objects contributing to the level spin; specific shell model configurations are also indicated. The odd-parity four-particle one-hole states of column 3 involve four configurations, with $\pi h^2 \nu f^2$ or $\nu f h$ coupled, respectively, with either the $\pi d_{5/2}^{-1}$ or $\pi g_{7/2}^{-1}$ hole, and analogous even-parity configurations occur in column 4, but here with one of the neutrons in $i_{13/2}$. Only the three highest yrast states of the two highest spin families $\pi h^2 \nu f h \pi g^{-1}$ and $\pi h^2 \nu h i \pi g^{-1}$ can be recognized from the data with some confidence. All ^{147}Eu states of columns 1–4 include in their configuration a 0^+ valence proton-hole pair, and they should thus occur similarly in the isotone ^{149}Tb (see Fig. 3 below). The levels of column 5 are specific for ^{147}Eu only since here all valence protons contribute to the spin. Levels of ambiguous energy are labeled with a dagger.

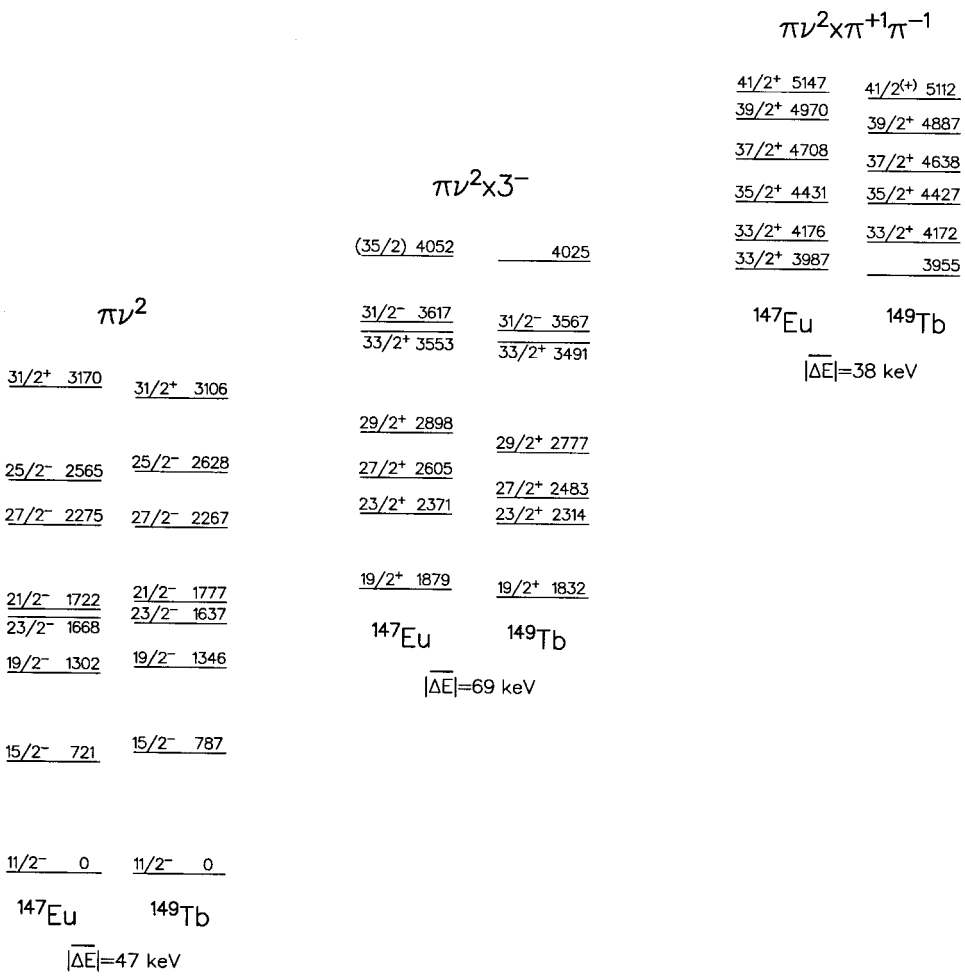

FIG. 3. Comparison between experimental high spin states in the $N=84$ isotones ^{147}Eu and ^{149}Tb [2]. The level energies are given relative to the $\pi h_{11/2}$ $11/2^-$ isomers, which lie at 625 keV in ^{147}Eu and at 36 keV in ^{149}Tb. Average energy deviations between the two isotones are given for the three groups of levels.

isotones. The preferred parities shown in parentheses in Fig. 2 derive from structural arguments discussed below.

Before detailed discussion of the results we mention that our level scheme largely confirms the pertinent conclusions of the previous in-beam studies [6–8]. We also confirm the findings of the parallel high spin work by Zhou *et al.* [9] up to their 41/2 state at 5.77 MeV. Above that energy there is no correspondence between levels; we do however observe all their γ rays from this region but place them differently in the scheme. Moreover our experiment with the GASP array provided much higher detection sensitivity. Below 5.8 MeV we identified more than twice as many states, most of them with spins and often also parities specified.

IV. DISCUSSION

In our experiment we find that the entire ^{147}Eu γ-ray flux proceeds ultimately through the $11/2^-$ isomer that lies at 625 keV excitation, and in fact it is a result of our study that in all the levels observed—with a single exception—the $h_{11/2}$ proton shell contributes to the level spin. Consequently, the low lying states will involve a 0^+ two-proton hole pair in their configurations, and we find that this is the case for almost all observed states up to 8 MeV. In the next sections we will proceed to discuss the ^{147}Eu levels in order of increasing structural complexity as they are arranged in the level scheme of Fig. 2.

A. Three-particle excitations

Above the $11/2^-$ isomer, the three lowest states represent the stretched couplings of the $h_{11/2}$ proton with the 2^+, 4^+, and 6^+ states of the two $f_{7/2}$ neutrons. Of the remaining 23 partially aligned members of this family we observe in our experiment only a single one, the $I_{\max}-1$ $21/2^-$ state, 54 keV above the fully aligned $23/2^-$ state at 2293 keV. But other members of the family are known from the literature (see Sec. V and Fig. 5 below).

We remark that the three lowest yrast level spacings above the $11/2^-$ state deviate significantly from the theoretical expectation obtained with a pure short-range two-body interaction. This observation directly relates to the spacings of the $(\nu f_{7/2}^2)_{0^+,\ldots,6^+}$ sequence as observed in ^{148}Gd and ^{146}Sm. There, the 2^+ energy is less than half the energy of the maximum aligned 6^+ state, much in contrast to the value of three-quarters calculated with a δ interaction for the 2^+ state in a j^2 energy spectrum. More detailed evaluation of the ^{148}Gd $\nu f_{7/2}^2$ energies is given in Ref. [1].

Lifting one neutron into the $h_{9/2}$ orbital can provide states up to $27/2^-$, which is the next higher yrast state at 2900 keV. In such a three-particle configuration of three different orbitals the maximum aligned state in general lies well below the lowest levels of neighboring spins and thus competes favorably for the yrast line, and in many cases it is the only state of the configuration seen in a heavy ion experiment. For the

$25/2^-$ member, observed here 290 keV above, the comparison with ^{149}Tb would suggest an assignment as the lower energy member of the $I_{\max}-1$ mixed symmetry doublet in the elementary S_3 group formed by this configuration of three distinguishable particles with (nearly) equal spins and interactions [2]. Also here, as in ^{149}Tb, the state decays through a 0.3 MeV intraconfiguration $M1$ transition to the $27/2^-$ fully aligned state, while 0.9 MeV interconfiguration $M1$ decay to the maximum aligned $(\pi h_{11/2}\nu f^2_{6^+})23/2^-$ state does not compete. However, in ^{147}Eu one anticipates a more complex nature for the $25/2^-$ state since here—in contrast to ^{149}Tb—additional $25/2^-$ excitations should occur nearby. We will return to this topic below when we discuss the 346 keV additional $25/2^-$ γ decay branch, which is absent in ^{149}Tb.

Promoting the $h_{9/2}$ neutron into the $i_{13/2}$ orbital will again provide two more units of angular momentum and a change in parity. The $31/2^+$ state at 3795 keV decaying through an octupole state via the 272 keV $M1-623$ keV $E1$ two-transition cascade to $27/2^-$ is assigned as this configuration, also on account of the identical feeding and decay branches as observed in ^{149}Tb. However, a second $31/2^+$ state, of $(\pi h_{11/2}j^{-2}_{0^+}\nu f_{7/2}h_{9/2}\times 3^-)I_{\max}-1$ character, is expected close in energy. The two states could well admix, and we observe probably only the lower one. The γ decay data do not distinguish the two alternatives. The next higher spin three-particle excitation, $(\pi h_{11/2}j^{-2}_{0^+}\nu h_{9/2}i_{13/2})33/2^+$, is expected to lie above 5 MeV, outside the range where our experiment identifies 33/2 states.

For the seven observed three-particle states the average deviation from terbium is 47 keV, and the average energy shift -18 keV (see Fig. 3).

B. Three-particle × octupole excitations

The even-parity levels of the second column of Fig. 2 are octupole core excitations coupled to the two lower three-particle configurations of column 1. The states up to $29/2^+$ at 3523 keV are of $(\pi h_{11/2}j^{-2}_{0^+}\nu f^2_{7/2}\times 3^-)$ character and the next higher state, at 4178 keV, is the aligned $(\pi h_{11/2}j^{-2}_{0^+}\nu f_{7/2}h_{9/2}\times 3^-)33/2^+$ excitation. Analogous octupole configurations are also known in terbium, at quite similar energy, but in contrast to terbium one notes that in europium $E1$ decay to the three-particle states is more favored, such that the low lying members of the octupole family $(\pi h_{11/2}j^{-2}_{0^+}\nu f^2_{7/2}\times 3^-)17/2^+$ and $15/2^+$ are completely bypassed in the ^{147}Eu yrast cascade. To us there is no obvious reason for this distinct difference, but it is known that the trend continues when one goes toward lower-Z isotones. In principle $\sim$0.6 MeV $M1$ decay would also be possible for the $I<25/2^+$ ^{147}Eu octupole levels to the known $(\pi d^{-1}_{5/2}\nu f^2_{7/2})$ or $(\pi g^{-1}_{7/2}\nu f^2_{7/2})$ states (see Ref. [7] and Fig. 4), but no such transitions with intensities above 0.5 units of Table I could be detected.

Above the firm $(\pi h_{11/2}j^{-2}_{0^+}\nu f_{7/2}h_{9/2}\times 3^-)33/2^+$ octupole state, three further ^{149}Tb levels have been proposed to have octupole nature [2], and their counterparts in ^{147}Eu are the states at 4242 keV with $I^\pi=31/2^-$, 4612 keV $(33/2^+)$, and 4677 keV (35/2), where the $31/2^-$ state was tentatively assigned in ^{149}Tb as the $(\pi h_{11/2}\nu f^2_{7/2}\times 3^-\times 3^-)I_{\max}-2$ double-octupole state. The newly determined even parity for the $33/2^+$ level at 4612 keV is incompatible with an octupole assignment but rather suggests a nonstretched $5qp$ nature, and the level is therefore placed in the next right column in Fig. 2. In contrast to ^{149}Tb the state has an additional intense decay branch, by a 328 keV dipole transition to a second $31/2^-$ level at 4284 keV. This latter state has no counterpart in ^{149}Tb, and as we will discuss below can occur only in ^{147}Eu. From the shell model we assign it as a proton one-particle two-hole neutron two-particle excitation (cf. preceding section and Sec. V).

All the octupole states lie consistently above their terbium partners in energy; for the five firmly assigned even-parity states the average upward shift is $+82$ keV. The shift relates to the increase of the core phonon energy from 1580 to 1810 keV when going from ^{146}Gd to ^{144}Sm.

We assign the $23/2^-$ level at 2845 keV as the stretched state of $(\pi d^{-1}_{5/2}\nu f^2_{7/2}\times 3^-)$ character. The state cannot belong to the $(\pi h_{11/2}j^{-2}_{0^+}\nu f_{7/2}h_{9/2})$ family where $23/2^-$ is expected ca. 250 keV above its fully aligned $27/2^-$ member (see Fig. 5), and also assignment as a second $(\pi h_{11/2}j^{-2}_{0^+}\nu f^2_{7/2}\times 3^-)$ state is unacceptable since the two lowest $23/2^+$ members of this configuration should be separated by about 500 keV [2]. Our assignment is based on the agreement with the shell model prediction (Sec. V C), and the level parity is thus from theory. Characteristic is the γ decay of this aligned $(\pi d^{-1}_{5/2}\nu f^2_{6^+}\times 3^-)23/2^-$ level exclusively to the $I_{\max}-1$ $(\pi h_{11/2}j^{-2}_{0^+}\nu f^2_{7/2})21/2^-$ state at 2347 keV. Having in mind the antialigned $(\pi h_{11/2}d^{-1}_{5/2})$ principal particle-hole component of the 3^- phonon, it becomes apparent that the 498 keV $M1$ deexcitation proceeds by sheer nucleon reorientation within the identical configuration, which also readily explains the absence of a decay to the 2293 keV $23/2^-$ level. The nature of the 346 keV feeding $(M1)$ transition is not immediately apparent, but the emitting $(\pi h_{11/2}j^{-2}_{0^+}\nu h_{9/2}f_{7/2})25/2^-$ state might well admix with $(\pi g^{-1}_{7/2}\nu f^2_{7/2}\times 3^-)25/2^-$, not observed in experiment but predicted at 2975 keV (see Fig. 5). The 346 keV γ ray could then proceed as $\pi g^{-1}_{7/2}\rightarrow\pi d^{-1}_{5/2}$. This 2845 keV $23/2^-$ octupole state, moreover, is the aforementioned single observed state where the $h_{11/2}$ proton does not explicitly contribute to the level spin. But here also $23/2^-$ states from other configurations are expected close in energy and will probably admix (Sec. V D).

C. Five-quasiparticle excitations

The levels of column 3 and to the right in Fig. 2 must all be composed of at least five valence nucleons. The lowest of these is the 4284 keV $31/2^-$ state mentioned above. It definitely has no counterpart in terbium and must therefore involve the breaking of the 0^+ proton-hole pair, which can provide spins 2 and 4, or up to 6 with one of the holes in the near lying $\pi g_{7/2}$ shell. Spin parity $31/2^-$ can be formed by $(\pi d^{-2}_{5/2})_{4^+}\times(\pi h_{11/2}\nu f^2_{7/2})_{23/2^-}$ or, more likely, by

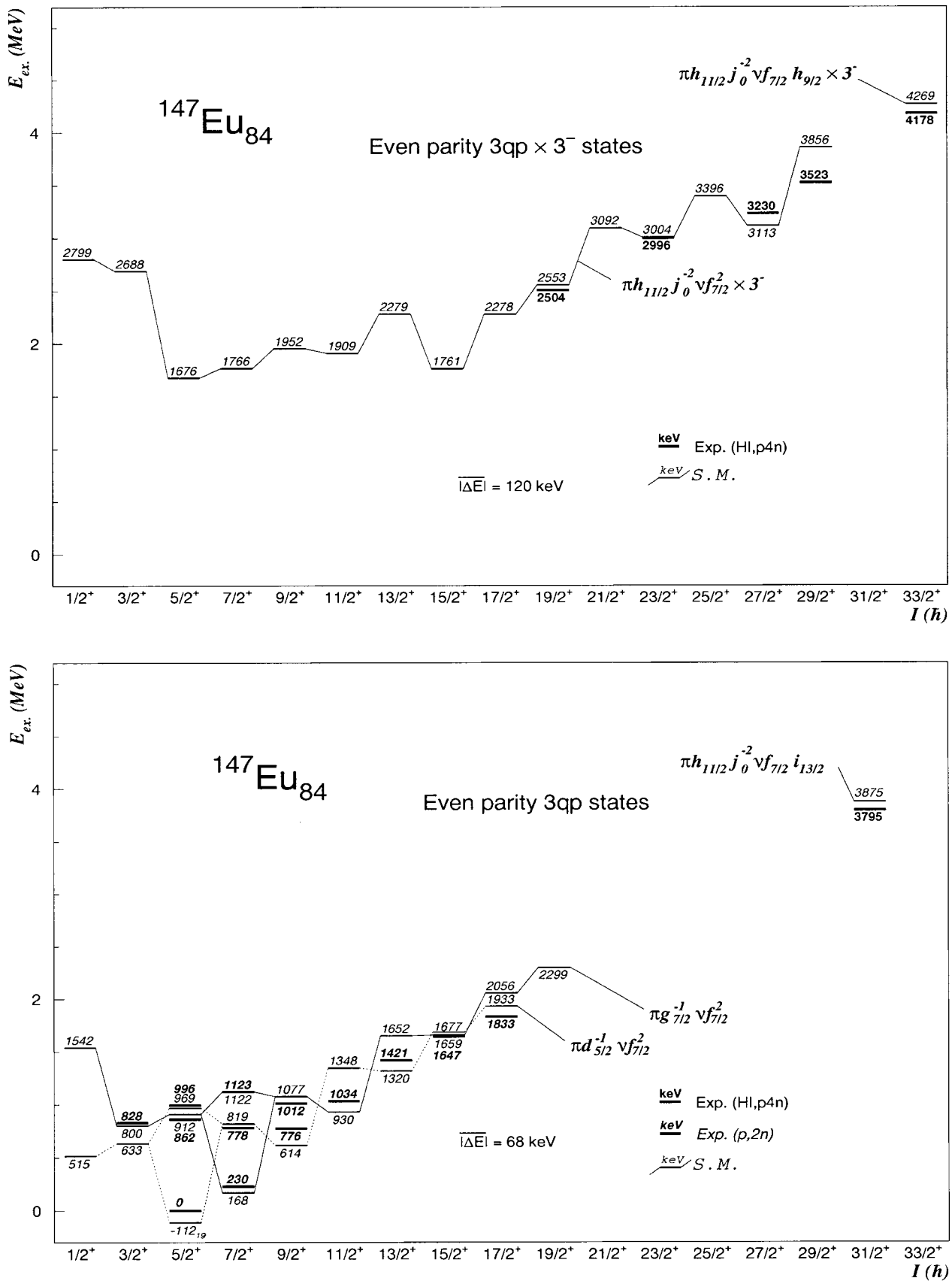

FIG. 4. Level energies calculated from the shell model (thin lines) compared with the assigned experimental states (solid bars), the latter marked with italic numbers when observed in the $(p,2n)$ reaction or in β decay. For each configuration only the calculated yrast levels are shown.

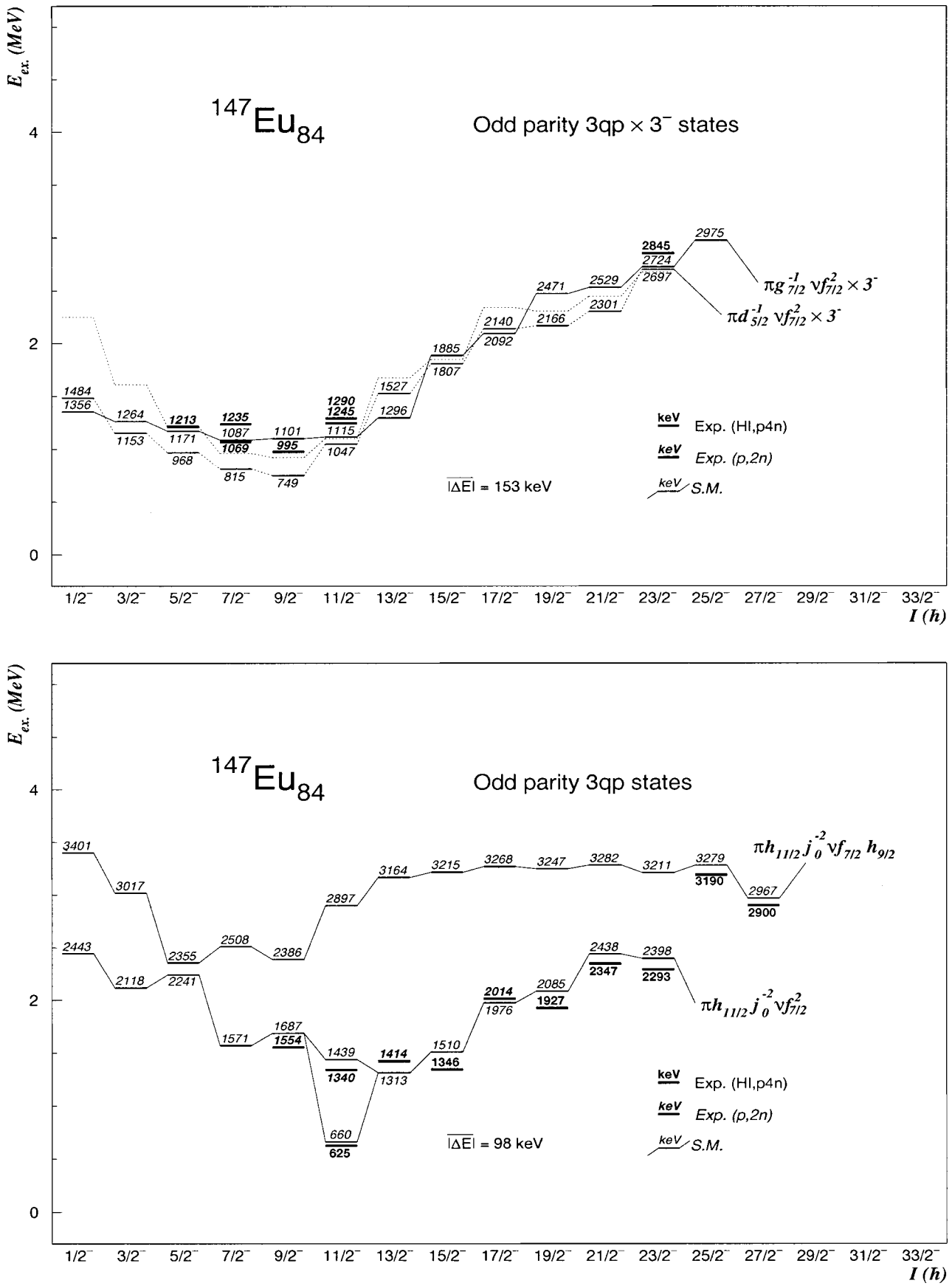

FIG. 5. The same as Fig. 4 for negative parity levels. The purely dotted line in the upper panel was calculated with the ($\pi h_{11/2}, \nu f_{7/2} \times 3^-$) exchange strength extracted from the septet data for ^{147}Tb (see Sec. V C).

$(\pi d_{5/2}^{-1} g_{7/2}^{-1})_{6^+} \times (\pi h_{11/2} \nu f_{7/2}^2)_{23/2^-}$, since here the inherent attraction of the aligned $(\pi d_{5/2}^{-1} g_{7/2}^{-1})_{6^+}$ singlet coupling will preferentially contribute to the configuration yrast states at higher spins. Our assignment as $I_{\max} - 2(\pi h_{11/2} d_{5/2}^{-1} g_{7/2}^{-1} \times \nu f_{7/2}^2) 31/2^-$ is strongly supported by the shell model results presented in Sec. V, where we will consider further possible assignments.

Among the other levels in this region we clearly identify a sequence of five monotonic $\Delta I = 1$ levels from $33/2^+$ to $41/2^+$ with characteristic high energy $E2$ decay, and evident counterparts in ^{149}Tb. Both the average excitation energy deviation and shift for these states are $+39$ keV. These levels are five-quasiparticle excitations involving promotion of a core proton across $Z = 64$ into $h_{11/2}$. For ^{149}Tb they could be calculated [2] as couplings of the $d_{5/2}$ or $g_{7/2}$ proton hole with the four-particle clusters $(\pi h_{11/2}^2 \nu f_{7/2}^2)_{16^+}$ or $(\pi h_{11/2}^2 \nu f_{7/2} h_{9/2})_{18^+}$ observed in ^{148}Dy, using in the decomposition the excitation energies of the contributing four-, three-, and two-body substructures as observed in the respective neighboring nuclei. For ^{147}Eu the corresponding data are not available, and we therefore base our assignments on the analogy with the isotone. The highest spin states of these configurations are pushed up in energy due to the repulsive interaction in the aligned coupling of the hole with the four particles. The above calculation [2] thus predicts that the fully aligned $(\pi h_{11/2}^2 g_{7/2}^{-1} \nu f_{7/2} h_{9/2}) 43/2^+$ state, unobserved in ^{149}Tb, should lie 428 keV above the $I_{\max} - 1\, 41/2^+$ level of the same configuration. In our data we clearly observe a 562 keV stretched magnetic dipole transition feeding the $41/2^+$ state, which we assign as the expected intraconfiguration $M1$ transition.

The less clearly characterized levels from 4.6 to 5.5 MeV shown to the right in Fig. 2 could well be members of these four five-quasiparticle configurations. But the very large number of levels in the spin range from 33/2 to 39/2 expected below the $41/2^+$ state prevents classification of individual levels.

On a more speculative level we propose a fully aligned $(\pi h_{11/2}^2 j_{0^+}^{-2} \nu h_{9/2} i_{13/2})_{21^-} \times \pi g_{7/2}^{-1}$ assignment for the firm 49/2 level at 7682 keV. This suggestion is in accordance with the feeding of the state through only high energy γ rays, and with its decay expected to proceed through a single $M1$ transition of intraconfigurational character. The only structural difference of this 49/2 state when compared with the $43/2^+$ state at 6333 keV is the excitation of the $f_{7/2}$ neutron particle, present in $(\pi h_{11/2}^2 j_{0^+}^2 \nu f_{7/2} h_{9/2})_{18^+}$, to the $\nu i_{13/2}$ orbit occupied in the 21^- four-particle complex of the 49/2 level.

In either of these two $\pi^2 \nu^2 \times \pi^{-1}$ four-particle one-hole configurations the aforementioned strong residual repulsion of the proton hole with the four aligned particles is gradually relaxed by dealignment of the hole. In all probability the repulsive high j two-body interactions of the proton hole with either the $\nu f_{7/2}$ or $\nu i_{13/2}$ particle are very much alike, which will result in quite similar yrast energy spectra for the two five-nucleon configurations. In the present data this is clearly evident from the comparison of the two highest $M1$ dealignment transitions, 513–202 keV from $49/2^{(-)}$ at 7682 keV, and 562–177 keV from $43/2^+$ at 6333 keV. With decreasing alignment the number of levels for each spin will increase rapidly and no clear decay patterns will prevail.

The considerations put forward above would also suggest that the two bare four-particle 18^+ and 21^- clusters in ^{148}Gd should have the same energy separation as their counterparts in ^{147}Eu. In fact they are known [1] in ^{148}Gd at 5833 and 7156 keV, 26 keV less separated than the 1349 keV spacing from $43/2^+$ to 49/2 in ^{147}Eu.

The most perturbing problem with these latter proposed assignments is the undetermined level parities. The four high energy implied $E1$ transitions, with 738, 892, 942, and 633 keV, all have quite accurate DCO values near 0.5, like the other four firmly assigned stretched $E1$ transitions in the scheme. But, as mentioned above, of the dipole transitions in Table I with energies above 500 keV only two have ratios firmly above 0.5 favoring mixed $M1 + E2$ character, while all others have ratios including 0.5 and therefore cannot specify the relative parities of the connected states. Without more conclusive data the configuration assignments above 6.5 MeV will thus remain speculative.

D. Seven-quasiparticle excitations

With $I = 49/2$ the expected valence spin for three protons and two neutron particles is exhausted, and the states above must be seven-quasiparticle states where all three proton holes in $d_{5/2}$ or $g_{7/2}$ will now contribute to the spin. The four states near 8.7 MeV thus could well have sizable components of $(\pi d_{5/2}^{-2})_{2^+}$, and the two below lying marginally characterized monopode levels (7420 and 6963 keV) are probably similar $\pi_{2^+}^{-2}$ excitations on five-quasiparticle states with lower neutron spin. Clearly these states are specific for ^{147}Eu since they exploit the angular momentum of the two proton holes not present in ^{149}Tb.

V. SHELL MODEL CALCULATIONS

Our shell model calculations are strictly limited to evaluation of the angular momentum recoupling of quantal particles. All the contributing dynamic quantities—single-particle energies and two-body interactions—we take from experiment, viz., from the excitation energies observed in the respective neighboring one- and two-body nuclei. Consequently, the results are in principle parameter free. As in general in such calculations, all our results ignore configuration mixing since the interconfigurational—off diagonal—matrix elements are not easy to observe in experiment. For the calculation we used a sufficiently elementary code based on fractional parentage recoupling which easily also calculates fermion-boson coupling. The code was originally developed by M. C. Bosca and was first used in [2].

A particular problem for the ^{147}Eu shell model calculations relates to the fact that almost all observed states involve in their configuration a 0^+ proton-hole pair. The fermion-boson interaction is then accounted for by taking all pertinent input quantities from nuclei where the 0^+ boson is present, and the calculation is then formally carried out as for the three-particle nucleus ^{149}Tb but now with ^{144}Sm as a core instead of ^{146}Gd. In ^{146}Eu, however, the proton-particle

neutron-particle multiplets lie at significantly higher excitation and are less well known than in ^{148}Tb, and for many two-nucleon states we therefore had to estimate the excitation energies in ^{146}Eu. These estimated values are included in Table II, and in some cases we will comment on them below.

Our recoupling calculations are usually limited to configurations with up to four objects and thus the matrix dimensions will not exceed 20. These configurations form the ^{147}Eu high spin states up to 33/2 near 4.2 MeV excitation, and they cover the three valence nucleons of ^{147}Eu in the available high spin orbitals and their couplings to the 3^- and 0^+ bosons. We also present examples for the recoupling of five objects, in these cases all fermions. In the comparison with experiment we will also consider ^{147}Eu levels observed in β decay [4] and in $(p,2n)$ in-beam experiments [6,7] which identified important lower spin states up to 2 MeV that provide a crucial test of theory and are not accessible in a heavy ion reaction.

Our calculated results are shown in Fig. 4 for even and Figs. 5 and 6 for odd parities. For each configuration only the calculated configuration yrast states are shown. For configurations with two $f_{7/2}$ neutrons we include, for the spin j of the single proton, also the calculated first excited state of dominant $(\pi j \nu f^2_{2^+})$ character. Due to its typical $\sim$10% admixture of $(\pi j \nu f^2_{0^+})$ the state can be clearly identified from the single-proton transfer data [5].

A. The proton-hole two-neutron-particle configurations $\pi d^{-1}_{5/2}\nu f^2_{7/2}$ and $\pi g^{-1}_{7/2}\nu f^2_{7/2}$

These two configurations have no 0^+ proton-hole pair and therefore are calculated straightforwardly as two-particle one-hole states relative to ^{146}Gd. The interactions for the two $f_{7/2}$ neutrons are taken from the four lowest 0^+ to 6^+ even-parity yrast levels of the two-neutron nucleus ^{148}Gd. The proton-hole neutron-particle interactions come from ^{146}Eu [13], where the complete $(\pi d^{-1}_{5/2}\nu f_{7/2})$ sextet is known and seven of the eight $(\pi g^{-1}_{7/2}\nu f_{7/2})$ states were identified; the missing 0^- energy is estimated, but it contributes only to the four calculated $7/2^+$ three-particle energies and negligibly to the lowest one.

The ^{147}Eu energies are then calculated from the respective excitation energies and ground state masses. The single fully aligned $(\pi d^{-1}_{5/2}\nu f^2_{7/2})17/2^+$ state, for example, is calculated from the data of Table II as

$$E^{^{147}\mathrm{Eu}}_{d^{-1}_{5/2}f^2_{7/2},17/2^+} = E^{^{148}\mathrm{Gd}}_{f^2_{6^+}} + \tfrac{19}{12}E^{^{146}\mathrm{Eu}}_{d^{-1}f_{6^+}} + \tfrac{5}{12}E^{^{146}\mathrm{Eu}}_{d^{-1}f_{5^+}} - 2E^{^{147}\mathrm{Gd}}_{f_{7/2}} - E^{^{145}\mathrm{Eu}}_{d_{5/2}} + S_{\pi^{-1}\nu^2} = 1933_{18}\ \mathrm{keV}$$

as shown in Fig. 4, 100 keV above experiment. The S value contains the pertinent six ground state masses and becomes, with the values of Table II

$$S_{\pi^{-1}\nu^2} = -M^{^{147}\mathrm{Eu}} + M^{^{148}\mathrm{Gd}} + 2M^{^{146}\mathrm{Eu}} - 2M^{^{147}\mathrm{Gd}} - M^{^{145}\mathrm{Eu}} + M^{^{146}\mathrm{Gd}} = -341_{18}\ \mathrm{keV},$$

and is the same for all calculated $\pi^{-1}\nu^2$ configurations in ^{147}Eu. The 18 keV error reflects the experimental errors of the six contributing ground state masses. For the—altogether 17—states with $I<17/2$ the code calculates and diagonalizes the interaction matrix for each spin, but as mentioned we include in the figures only the nine resulting yrast states of the configuration and the first above-yrast state with spin 5/2. Analogous calculations give the respective theoretical energies for $(\pi g^{-1}_{7/2}\nu f^2_{7/2})$ also included in Fig. 4.

Of all these states we see none in our experiment, not even the ^{147}Eu ground and first excited states, since the 0.77 μs half-life strongly reduces observation of the γ rays below it. Many of these levels, ranging up to a $17/2^+$ yrast state at 1833 keV, are, however, populated in the $(p,2n)$ experiments [6,7] or in β decay [4] and can be quite firmly assigned to these two configurations (cf. Fig. 4). In most cases the assignments are strongly supported by the γ-ray feeding and deexcitation patterns.

We remark here that we have modified the spin assignment for three even-parity levels tentatively characterized [7] in $(p,2n)$ as 862 keV $(7/2)^+$, 996 keV $(1/2)^+$, and 1123 keV $(9/2)^+$. The subsequent ^{148}Gd(t,α) single-proton pickup experiment [5] gave $l=2$ for the two former and $l=4$ transfer for the latter state, which firmly establishes their spin parities $5/2^+$, $5/2^+$, and $7/2^+$, respectively, and we assign the states as $(\pi g^{-1}_{7/2}\nu f^2_{2^+})5/2^+$, $(\pi d^{-1}_{5/2}\nu f^2_{2^+})5/2^+$, and $(\pi g^{-1}_{7/2}\nu f^2_{2^+})7/2^+$ as shown in Fig. 4. Moreover the new spin assignments are in much better agreement with the γ decays, avoiding low energy $E2$ and $M3$ competition with $M1$ radiation of much higher energy.

Two $3/2^+$ states were seen in the $(p,2n)$ experiment, at 755 and 828 keV, where transfer data [5] favor the $d^{+1}_{3/2}$ proton-particle assignment [14] for the 755 keV state discussed in the next section. The γ decay of the 828 keV $3/2^+$ level is unspecific, but we assign the state as $(\pi g^{-1}_{7/2}\nu f^2_{2^+})$ on account of the closely calculated energy. There is then, however, no candidate for the $3/2^+$ yrast state of $(\pi d^{-1}_{5/2}\nu f^2_{2^+})$ character, which should lie below.

The comparison in Fig. 4 of the shell model predictions with experiment for these two configurations gives the average values for energy deviation and energy shift of $\overline{|\Delta E|}=91$ and $\overline{|\Delta E|}=+44$ keV for the six assigned $(\pi d^{-1}_{5/2}\nu f^2_{7/2})$ levels, and $\overline{|\Delta E|}=69$ and $\overline{|\Delta E|}=+15$ keV for the seven $(\pi g^{-1}_{7/2}\nu f^2_{7/2})$ states. These states include all even-parity levels observed in $(p,2n)$ except for the just mentioned $\pi d_{3/2}$ state at 755 keV.

B. The one-proton-particle two-neutron-particle configurations

The low lying proton-particle states are $\pi s_{1/2}$, $\pi h_{11/2}$, and $\pi d_{3/2}$. In ^{147}Eu they are formed by lifting one proton across $Z=64$ and thus involve the two-proton-hole 0^+ pair boson. Consequently we calculate the three-particle states relative to ^{144}Sm.

The odd-parity yrast levels up to $23/2^-$ observed in our experiment are of $(\pi h_{11/2}j^{-2}_{0^+}\nu f^2_{7/2})$ character. We now take the two-body states for the shell model calculation from

TABLE II. Input data used in the present shell model calculations. Asterisks indicate estimated values.

Nucleus	Configuration	I^π	E_x (keV) or mass excess [21]	Config. Assgt. Ref.
^{144}Sm	3^-	3^-	1810	[1]
	$\pi d_{5/2}^{-2}$	4^+	2190	[22]
		2^+	1660	[22]
		0^+	$-81\,976_3$	[22]
	$\pi g_{7/2}^{-2}$	6^+	3079	[22]
		4^+	3020	[22]
		2^+	2800	[22]
		0^+	(2478)	[22]
	$\pi d_{5/2}^{-1} g_{7/2}^{-1}$	6^+	2323	[22]
		5^+	2707	[22]
		4^+	2588	[22]
		3^+	2687	[22]
		2^+	2661	[22]
		1^+	2645	[22]
^{145}Sm	$\pi_{0^+}^{-2} \nu f_{7/2}$	$7/2^-$	$-80\,662_3$	SM
	$\pi_{0^+}^{-2} \nu h_{9/2}$	$9/2^-$	1423	[23]
	$\pi_{0^+}^{-2} \nu i_{13/2}$	$13/2^+$	2100	[1]
	$\pi_{0^+}^{-2} \nu f_{7/2} \times 3^-$	$13/2^+$	1105	[24]
		$11/2^+$	1966	[25]
		$9/2^+$	1848	[24]
		$7/2^+$	1858	[24]
		$5/2^+$	1804	[24]
		$3/2^+$	1628	[24]
		$1/2^+$	1436	[24]
^{146}Sm	$\pi_{0^+}^{-2} \nu f_{7/2}^2$	6^+	1812	[1]
		4^+	1381	[1]
		2^+	747	[1]
		0^+	$-81\,006_4$	[1]
	$\pi_{0^+}^{-2} \nu f_{7/2} h_{9/2}$	8^+	2737	[1]
		7^+	2912	*[a]
		6^+	2826	*[a]
		5^+	2903	*[a]
		4^+	2882	*[a]
		3^+	2913	*[a]
		2^+	2789	*[a]
		1^+	2893	*[a]
	$\pi_{0^+}^{-2} \nu f_{7/2} i_{13/2}$	10^-	3754	[1]
	$\pi_{0^+}^{-2} \nu f_{7/2} h_{9/2} \times 3^-$	11^-	3783	[1]
^{145}Eu	$\pi d_{5/2}^{-1}$	$5/2^+$	$-78\,002_4$	SM
	$\pi g_{7/2}^{-1}$	$7/2^+$	330	SM
	$\pi_{0^+}^{-2} \pi h_{11/2}$	$11/2^-$	716	SM
	$\pi_{0^+}^{-2} \pi h_{11/2} \times 3^-$	$17/2^+$	(3187)	[19,26]
		$15/2^+$	2245	[19,26]
		$13/2^+$	2897	[19,26]
		$11/2^+$	2470	*[19,26]
		$9/2^+$	(2617)	[19,26]
		$7/2^+$	2520	*[19,26]
		$5/2^+$	2530	*[19,26]
^{145}Eu	$\pi d_{5/2}^{-1} \times 3^-$	$11/2^-$	1602	[19,26]
		$9/2^-$	1368	[19,26]
		$7/2^-$	1500	[19,26]
		$5/2^-$	(1567)	[19,26]
		$3/2^-$	1600	[19,26]
		$1/2^-$	1700	*[b]
	$\pi g_{7/2}^{-1} \times 3^-$	$13/2^-$	1845	[19,26]
		$11/2^-$	1792	[19,26]
		$9/2^-$	1827	[19,26]
		$7/2^-$	1745	[19,26]
		$5/2^-$	1766	[19,26]
		$3/2^-$	1762	[19,26]
		$1/2^-$	1750	*[b]
^{146}Eu	$\pi d_{5/2}^{-1} \nu f_{7/2}$	6^-	289	[27]
		5^-	14	[27]
		4^-	$-77\,128_7$	[27]
		3^-	115	[27]
		2^-	230	[27]
		1^-	(1210)	[27]
	$\pi g_{7/2}^{-1} \nu f_{7/2}$	7^-	648	[27]
		6^-	373	[27]
		5^-	316	[27]
		4^-	331	[27]
		3^-	421	[27]
		2^-	498	[27]
		1^-	385	[27]
		0^-	2500	*[c]
	$\pi_{0^+}^{-2} \pi h_{11/2} \nu f_{7/2}$	9^+	666	[27]
		8^+	1201	[27]
		7^+	915	[27]
		6^+	(1071)	[27]
		5^+	902	[27]
		4^+	(934)	[27]
		3^+	840	[27]
		2^+	753	[27]
	$\pi_{0^+}^{-2} \pi d_{3/2} \nu f_{7/2}$	5^-	1036	*[d]
		4^-	1287	*[d]
		3^-	1405	*[d]
		2^-	(691)	[27]
	$\pi_{0^+}^{-2} \pi s_{1/2} \nu f_{7/2}$	4^-	(784)	[27]
		3^-	870	*[d]
	$\pi_{0^+}^{-2} \pi h_{11/2} \nu h_{g/2}$	10^+	2060	*[e,f]
		9^+	2299	*[e]
		8^+	2230	*[e]
		7^+	2266	*[e]
		6^+	2186	*[e]
		5^+	2246	*[e]
		4^+	2126	*[e]
		3^+	2146	*[e]
		2^+	1706	*[e]
		1^+	1196	*[e]
	$\pi_{0^+}^{-2} \pi h_{11/2} \nu i_{13/2}$	12^-	2628	*[g]

TABLE II. (*Continued*.)

Nucleus	Configuration	I^π	E_x (keV) or mass excess [21]	Config. Assgt. Ref.	Nucleus	Configuration	I^π	E_x (keV) or mass excess [21]	Config. Assgt. Ref.
	$\pi_{0^+}^{-2}\pi h_{11/2}\nu f_{7/2}$	12^-	2027	[27]		$\nu f_{7/2}\times 3^-$	$13/2^+$	997	[24]
	$\times 3^-$						$11/2^+$	1702	[1]
^{147}Eu	$\pi d_{5/2}^{-1}\nu f_{7/2}^2$	$5/2^+$	$-77\,555_4$	SM			$9/2^+$	1643	[1]
		$17/2^+$	1833	[7]			$7/2^+$	1628	[1]
^{146}Gd		0^+	$-76\,098_5$	SM			$5/2^+$	1627	[23]
	$\hbar\omega_3$	3^-	1579	[28]			$3/2^+$	1412	[24]
	$\pi d_{5/2}^{-1}h_{11/2}$	8^-	3183	[29]			$1/2^+$	1292	[24]
		7^-	2982	[29]	^{148}Gd	$\nu f_{7/2}^2$	6^+	1811	[1]
		6^-	3098	[29]			4^+	1416	[1]
		5^-	2658	[29]			2^+	784	[1]
		4^-	2997	[29]			0^+	$-76\,280_3$	[1]
		3^-				$\nu f_{7/2}^2\times 3^-$	9^-	2695	[1]
	$\pi g_{7/2}^{-1}h_{11/2}$	9^-	3428	[29]	^{147}Tb	$\pi h_{11/2}$	$11/2^-$	$-70\,708_{13}$	SM
		8^-	3293	[29]	^{148}Tb	$\pi h_{11/2}\nu f_{7/2}$	9^+	$-70\,430_{30}$	[17]
		7^-	3290	[29]			8^+	316	[17]
		6^-	3384	[29]			7^+	238	[17]
		5^-	3313	[29]			6^+	336	[17]
		4^-	(3412)	[29]			5^+	261	[17]
		3^-	(3389)	[29]			4^+	285	[17]
		2^-	(3660)	[29]			3^+	191	[17]
^{147}Gd	$\nu f_{7/2}$	$7/2^-$	$-75\,368_4$	SM			2^+	88	[17]

[a]Multiplet spacings of ^{148}Gd as listed in [2], but 7^+ member lowered by 66 keV as adopted in Ref. [15].
[b]Extrapolated.
[c]Energy estimated for an antialigned $T=0$ triplet S state.
[d]Multiplet spacings of ^{148}Tb [17].
[e]Multiplet spacings from ^{148}Tb as listed in [2].
[f]$(\pi h_{11/2}\nu h_{9/2})_{10+}$ to $(\pi h_{11/2}\nu f_{7/2})_{9+}$ separation taken from ^{148}Tb [2].
[g]Using $V((\pi h_{11/2}\nu i_{13/2})_{12^-})=-631$ keV deduced in [2] for ^{148}Tb.

^{146}Sm, with quite similar $\nu f_{7/2}^2$ energies as in ^{148}Gd, and from ^{146}Eu, where the $(\pi h_{11/2}\nu f_{7/2})$ octet lies at significantly higher excitation and is more affected by other levels than in the isotone ^{148}Tb. The energy of the $23/2^-$ highest spin state is calculated with the data from Table II as

$$E^{^{147}\mathrm{Eu}}_{h_{11/2}f_{7/2}^2,23/2-}=E^{^{146}\mathrm{Sm}}_{f_{6^+}^2}+\tfrac{25}{18}E^{^{146}\mathrm{Eu}}_{hf_{9^+}}+\tfrac{11}{18}E^{^{146}\mathrm{Eu}}_{hf_{8^+}}-2E^{^{145}\mathrm{Sm}}_{f_{7/2}}-E^{^{146}\mathrm{Eu}}_{h_{11/2}}$$

$$+S_{\pi^{+1}\pi_{0^+}^{-2}\nu^2}=2398_{16}\ \text{keV},$$

105 keV above experiment, where the mass term, valid for all $\pi^{+1}\pi_{0^+}^{-2}\nu^2$ three-particle configurations in ^{147}Eu, is

$$S_{\pi^{+1}\pi_{0^+}^{-2}\nu^2}=-M^{^{147}\mathrm{Eu}}+M^{^{146}\mathrm{Sm}}+2M^{^{146}\mathrm{Eu}}-2M^{^{145}\mathrm{Sm}}-M^{^{145}\mathrm{Eu}}$$

$$+M^{^{144}\mathrm{Sm}}=-357_{16}\ \text{keV}.$$

The energies for the 26 lower spin states are obtained from matrix diagonalization. The calculation is compared to experiment in Fig. 5. The $17/2^-$, $13/2^-$, and $9/2^-$ configuration yrast states and the second $11/2^-$ level are from the $(p,2n)$ data [7]. The latter $11/2^-$ state apparently [5] admixes to near-lying $11/2^-$ octupole states at 1245 and 1290 keV (Fig. 5), which makes individual configuration assignments problematic. For the nine observed states of the configuration the average deviation and shift compared with the theory are 101 and -66 keV.

To calculate the next higher odd-parity configuration $(\pi h_{11/2}\nu f_{7/2}h_{9/2})$, we need the $(\pi h_{11/2}\nu h_{9/2})$ two-body multiplet in ^{146}Eu, which is completely unknown, and similarly so the $\nu f_{7/2}\nu h_{9/2}$ family of ^{146}Sm except for its 8^+ member at 2737 keV [1]. In order to keep the philosophy of using only experimental interactions we presume, in accordance with lowest order expectation, that the level spacings for the corresponding particle-particle multiplets should be the same in the respective isotones. For ^{146}Sm we thus use the spacings of the $(\nu f_{7/2}\nu h_{9/2})$ octet in ^{148}Gd [2,15,16], shifted to match the ^{146}Sm$(\nu f_{7/2}\nu h_{9/2})8^+$ energy. The $(\pi h_{11/2}\nu h_{9/2})$ decet of ^{146}Eu likewise is taken from the ^{148}Tb [17] data, where the $9^+(\pi h_{11/2}\nu f_{7/2})$ energy was taken as a reference

for the excitation energy shifts. With these—somewhat forced—assumptions we calculate the two observed states of the configuration slightly above experiment with an average deviation and shift of +78 keV, and include in Fig. 5 the complete yrast line of this 71-level configuration.

For the next higher lying three-particle configuration $(\pi h_{11/2}\nu f_{7/2}i_{13/2})$ we calculate only the observed fully aligned $31/2^+$ state from the data of Table II as

$$E^{^{147}\mathrm{Eu}}_{h_{11/2}f_{7/2}i_{13/2},31/2^+} = E^{^{146}\mathrm{Eu}}_{hf_{9^+}} + E^{^{146}\mathrm{Eu}}_{hi_{12^-}} + E^{^{146}\mathrm{Sm}}_{fi_{10^-}} - E^{^{145}\mathrm{Eu}}_{h_{11/2}} - E^{^{146}\mathrm{Sm}}_{f_{7/2}} - E^{^{145}\mathrm{Sm}}_{i_{13/2}} + S_{\pi^{+1}\pi^{-2}_{0^+}\nu^2} = 3875_{17}\ \text{keV},$$

80 keV above the experiment (cf. Fig. 4).

Although in the present experiment we see only three-particle states involving the $h_{11/2}$ proton, we also have calculated the energies for the two even-parity $(\pi s_{1/2}j^{-2}_{0^+}\nu f^2_{7/2})$ and $(\pi d_{3/2}j^{-2}_{0^+}\nu f^2_{7/2})$ families using $\pi^{+1}\pi^{-2}_{0^+}\nu^{+1}$ two-body energies of ^{146}Eu largely estimated from the corresponding multiplet spacings observed in ^{148}Tb [17], and the ν^2 energies from ^{146}Sm as above. We calculate the $(\pi d_{3/2}j^{-2}_{0^+}\nu f^2_{0^+})$ state at 652 keV, 103 keV below the 755 keV experimental $3/2^+$ state [14], and the $(\pi s_{1/2}j^{-2}_{0^+}\nu f^2_{0^+})$ state as low as 480 keV. This latter state is still experimentally unknown, but in fact none of the performed experiments is suitable to identify a low lying $1/2^+$ particle state in ^{147}Eu. More importantly, the calculated results suggest that the $I>5/2$ states of the two three-particle families all should lie 0.5 to 1.2 MeV above the highest assigned states of the corresponding spins in Fig. 4.

C. Three-nucleon × octupole excitations

In the $N=84$ nuclei the ^{146}Gd 2^+ particle-hole phonon at 1972 keV very significantly admixes into the low-lying $\nu f^2_{7/2}2^+$ state near 0.78 MeV [18], and thus in our calculations is appropriately accounted for by using the observed $(\nu f^2_{7/2})_{2^+}$ energy. In contrast the two valence neutrons cannot provide a 3^- state below the core octupole phonon at 1580 keV. It therefore more evidently preserves its nature at $N=84$, and its coupling to the nucleons must be calculated explicitly.

The pertinent elementary two-body interactions are observed in the one-particle neighbors of ^{146}Gd where the respective particle × phonon multiplets to a large extent have been identified (cf. Table II). With these data the ^{147}Eu octupole excitations are obtained in a recoupling calculation for its three valence nucleons and the 3^- core boson, while the 0^+ boson, where applicable, is taken into account as described above.

Again we first consider configurations with the single proton hole in the $d_{5/2}$ or $g_{7/2}$ orbital below $Z=64$, which are calculated relative to the ^{146}Gd core. The additional two-body energies needed here are the $(\nu f_{7/2}\times 3^-)$ septet of ^{147}Gd and the $(\pi d^{-1}_{5/2}\times 3^-)$ and $(\pi g^{-1}_{7/2}\times 3^-)$ multiplets of ^{145}Eu.

In the ^{147}Gd septet the dominant anharmonicity is the very low energy of the $(\nu f_{7/2}\times 3^-)_{13/2^+}$ state, which is due to the strong interaction with the above-lying $\nu i_{13/2}$ single-particle state. The same interaction is also largely responsible [1] for the ≈0.3 MeV lowering of the 3^- phonon energy when going from $N=82$ to 84. Knowledge of the proton-hole × octupole multiplets is less complete; the energies listed in Table II were—quite tentatively—proposed [19] from γ-ray measurements.

The only state of $\pi^{-1}\nu^2\times 3^-$ character observed in the present experiment is the fully aligned four-particle structure $(\pi d^{-1}_{5/2}\nu f^2_{7/2}\times 3^-)_{23/2^-}$, and the calculation for this state proceeds as follows:

$$E^{^{147}\mathrm{Eu}}_{d^{-1}_{5/2}f^2_{7/2}\times 3^-,23/2^-} = \tfrac{20}{13}E^{^{147}\mathrm{Gd}}_{f\times 3_{13/2^+}} + \tfrac{6}{13}E^{^{147}\mathrm{Gd}}_{f\times 3_{11/2^+}} + E^{^{146}\mathrm{Eu}}_{d^{-1}\times 3_{11/2^-}} + \tfrac{19}{12}E^{^{146}\mathrm{Eu}}_{d^{-1}f_{6^+}} + \tfrac{5}{12}E^{^{146}\mathrm{Eu}}_{d^{-1}f_{5^+}} + E^{^{148}\mathrm{Gd}}_{f^2_{6^+}} - 2E^{^{146}\mathrm{Gd}}_{3^-} - 4E^{^{147}\mathrm{Gd}}_{f_{7/2}} - 2E^{^{145}\mathrm{Eu}}_{d_{5/2}} + S_{\pi^{-1}\nu^2} = 2697_{18}\ \text{keV},$$

148 keV below the observed energy. This state can alternatively be calculated by using in the reduction pertinent three-body substructures that have been observed in neighboring nuclei. Naturally, one would expect better results from such a less complex calculation, which proceeds as follows:

$$E^{^{147}\mathrm{Eu}}_{d^{-1}_{5/2}f^2_{7/2}\times 3^-,23/2^-} = E^{^{145}\mathrm{Eu}}_{d^{-1}\times 3_{11/2^-}} + E^{^{148}\mathrm{Gd}}_{f^2\times 3_{9^-}} + E^{^{147}\mathrm{Eu}}_{d^{-1}f^2_{17/2^+}} - E^{^{145}\mathrm{Eu}}_{d_{5/2}} - E^{^{148}\mathrm{Gd}}_{f^2_{6^+}} - E^{^{146}\mathrm{Gd}}_{3^-} + S = 2740\ \text{keV},$$

where S apparently is zero in this case. The result of this independent calculation is in reasonable agreement with the above value and now within 105 keV of the experiment. The remaining energy mismatch very probably arises from some expected mixing with the $(\pi h_{11/2}j^{-2}_{0^+}\nu f^2_{7/2})23/2^-$ state at 2293 keV (cf. Fig. 5), or also with the $(\pi h_{11/2}d^{-1}_{5/2}g^{-1}_{7/2}\nu f^2_{7/2})23/2^-$ five-nucleon state expected at 2900 keV (Sec. V D and Fig. 6).

The lower spin configuration yrast states of Fig. 5 are obtained with the pertinent sets of two-body energies in Table II analogous to the technique used above. A similar calculation gives the $(\pi g^{-1}_{7/2}\nu f^2_{7/2}\times 3^-)$ yrast levels also included in the figure. None of these latter states were observed in our reaction; the six experimental lower spin states shown in the figure come from radioactivity [4] and $(p,2n)$ studies [6,7].

A perturbing result is the low predicted energies for the $(\pi d^{-1}_{5/2}\nu f^2_{7/2}\times 3^-)$ states with spins below 13/2. Levels at these energies should very probably have been seen in experiment. The problem might arise from the $(\pi d^{-1}_{5/2}\times 3^-)$ sextet input energies of ^{145}Eu, some of which are not firmly characterized from the data. Here one expects [19] significant upward shift for the low spin sextet members, caused by

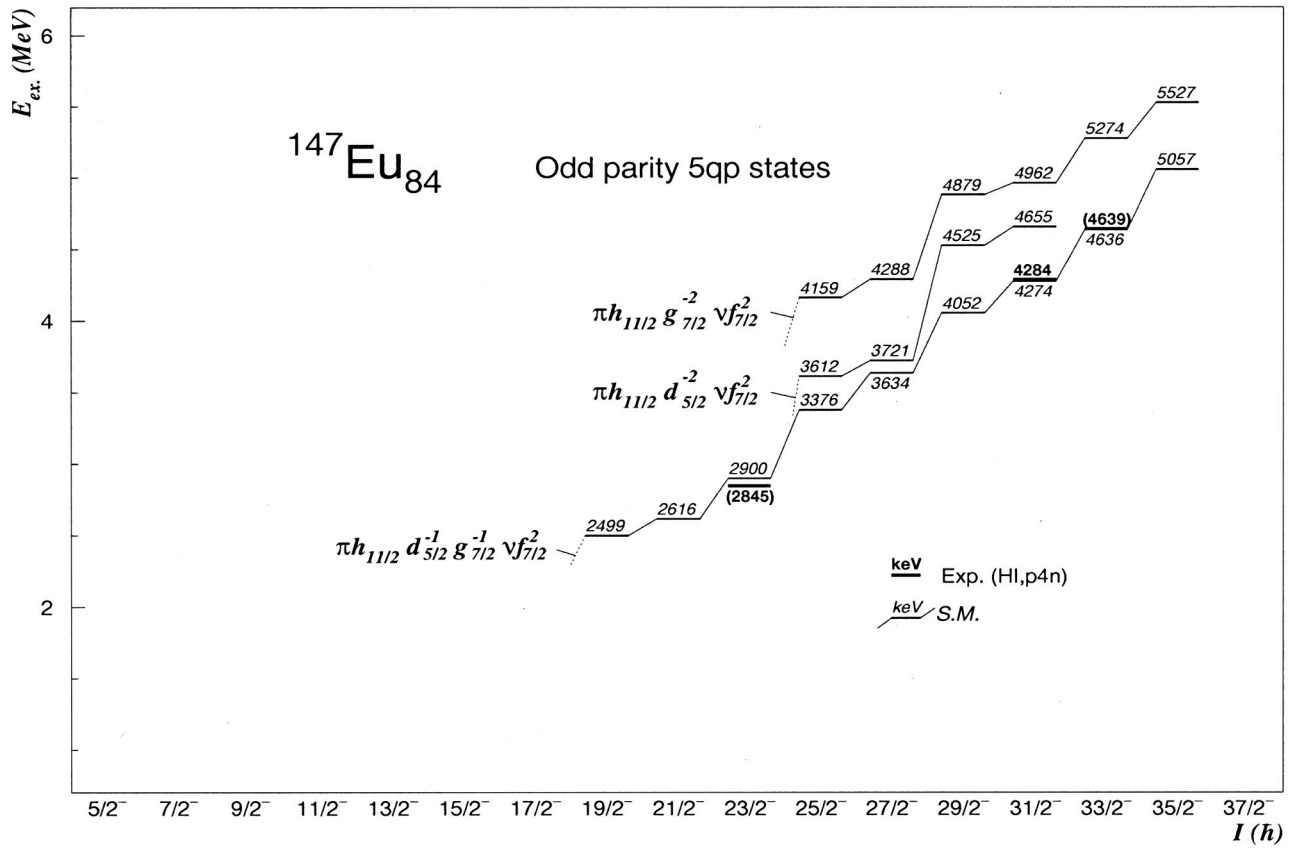

FIG. 6. Calculated configuration yrast for the $\pi^{+1}\pi^{-2}\nu^{+2}$ five-quasiparticle configurations compared to experimental results.

the exclusion principle from the exchange of a $d_{5/2}$ proton hole with the hole in the dominant $(\pi h_{11/2}d_{5/2}^{-1})$ octupole component, which is not obvious in experiment.

Using instead sextet energies calculated with the exchange strength, as extracted from the 772 keV energy splitting of the $17/2^+$ and $15/2^+$ $(\pi h_{11/2}\times 3^-)$ septet members of ^{147}Tb [19,20], the predicted ^{147}Eu $(\pi d_{5/2}^{-1}\nu f_{7/2}^{2}\times 3^-)$ energies for these low spin states move up much closer to experimental candidates. The results of this separate calculation are included in Fig. 5 as a dotted line. Comparable drastic anharmonicities are not anticipated for the $(\pi g_{7/2}^{-1}\times 3^-)$ septet energies since the $g_{7/2}$ proton hole plays no prominent role in the 3^- phonon, and the calculated $(\pi g_{7/2}^{-1}\nu f_{7/2}^{2}\times 3^-)$ octupole states of Fig. 5 should therefore be more reliable.

Comparison with theory gives the average deviation of $\overline{|\Delta E|}=200$ keV for these octupole states based on $\pi d_{5/2}^{-1}$, and $\overline{|\Delta E|}=128$ for those on $\pi g_{7/2}^{-1}$, where the former deviation would be much smaller with the alternative calculation.

The even-parity octupole excitations built on the $\pi h_{11/2}$ proton particle again include the 0^+ proton-hole pair and therefore are calculated relative to the ^{144}Sm core. In addition to the $\pi_{0^+}^{-2}\pi^{+1}\nu^{+1}$ and $\pi_{0^+}^{-2}\nu^2$ multiplets of ^{146}Eu and ^{146}Sm already used above, we now also need the fermion-boson septets $(\pi h_{11/2}j_{0^+}^{-2}\times 3^-)$ from ^{145}Eu and $(\pi j_{0^+}^{-2}\nu f_{7/2}\times 3^-)$ in ^{145}Sm. The latter septet is well known (see Table II) and quite similar to the $(\nu f_{7/2}\times 3^-)$ septet of ^{147}Gd discussed above. In ^{145}Eu only four septet states are known; the missing members were estimated from the theoretical relative shifts of this multiplet [19]. The dominant feature here is the very large diagonal repulsion of the aligned $17/2^+$ state. As in the $(\pi d_{5/2}^{-1}\times 3^-)$ sextet the shift here also arises from the exclusion principle [20], but now from the exchange of the $\pi h_{11/2}$ valence particle with the particle in the $(\pi h_{11/2}d_{5/2}^{-1})$ principal phonon component, where in maximum spin coupling both $\pi h_{11/2}$ particles would occupy the same quantum state. In the calculated $(\pi h_{11/2}j_{0^+}^{-2}\nu f_{7/2}^{2}\times 3^-)$ energies this $(\pi h_{11/2}\times 3^-)$ anharmonicity is reflected in a very large—743 keV—calculated spacing of the 29/2 and 27/2 highest spin yrast states of the configuration (cf. Fig. 4), in fact in poor agreement with the experiment where the difference is 297 keV only. The obvious origin of this shortcoming is the treatment in the calculation of the $(\nu i_{13/2},\nu f_{7/2}\times 3^-)$ interaction by perturbation only, via the low $(\nu f_{7/2}\times 3^-)13/2^+$ septet member energy of ^{145}Sm. The relative signs and magnitudes of the deviations are expected from this approximation in theory. For the two other states identified in the experiment the calculated energies agree much better.

Of the next higher three-particle $\times$ octupole configuration, $(\pi h_{11/2}j_{0^+}^{-2}\nu f_{7/2}h_{9/2}\times 3^-)$, we observe only the maximum aligned $33/2^+$ state, at 4178 keV, and calculate its energy from the three-, two-, and one-body substructures listed in Table II as

$$
\begin{aligned}
&E^{^{147}\mathrm{Eu}}_{h_{11/2}j^{-2}_{0^+}f_{7/2}h_{9/2}\times 3^-,33/2^+}\\
&\quad = E^{^{146}\mathrm{Eu}}_{hf\times 3_{12^-}} + E^{^{146}\mathrm{Sm}}_{fh\times 3_{11^-}} + E^{^{146}\mathrm{Eu}}_{hh_{10^+}}\\
&\qquad - E^{^{145}\mathrm{Sm}}_{f\times 3_{13/2^+}} - E^{^{145}\mathrm{Eu}}_{h_{11/2^-}} - E^{^{145}\mathrm{Sm}}_{h_{9/2^-}} + S_{\pi^{+1}\pi^{-2}_{0^+}\nu^2}\\
&\quad = 4269_{17}\ \text{keV},
\end{aligned}
$$

91 keV above experiment. For all even-parity octupole states the average deviation is 120 keV.

D. Five-quasipartricle excitations

As mentioned before we expect the lowest five-nucleon states to be of $(\pi h_{11/2}d^{-1}_{5/2}g^{-1}_{7/2}\nu f^2_{7/2})$ character, where all three protons contribute to the spin, and we calculate the fully aligned $35/2^-$ state from the shell model with the data of Table II as

$$
\begin{aligned}
&E^{^{147}\mathrm{Eu}}_{h_{11/2}d^{-1}_{5/2}g^{-1}_{7/2}f^2_{7/2},35/2^-}\\
&\quad = E^{^{146}\mathrm{Gd}}_{hd^{-1}_{8^-}} + E^{^{146}\mathrm{Gd}}_{hg^{-1}_{9^-}} + E^{^{144}\mathrm{Sm}}_{d^{-1}g^{-1}_{6^+}} + E^{^{148}\mathrm{Gd}}_{f^2_{6^+}} + \tfrac{25}{18}E^{^{148}\mathrm{Tb}}_{hf_{9^+}} + \tfrac{11}{18}E^{^{148}\mathrm{Tb}}_{hf_{8^+}}\\
&\qquad + \tfrac{19}{12}E^{^{146}\mathrm{Eu}}_{d^{-1}f_{6^-}} + \tfrac{5}{12}E^{^{146}\mathrm{Eu}}_{d^{-1}f_{5^-}} + \tfrac{3}{2}E^{^{146}\mathrm{Eu}}_{g^{-1}f_{7^-}} + \tfrac{1}{2}E^{^{146}\mathrm{Eu}}_{g^{-1}f_{6^-}}\\
&\qquad - 3E^{^{147}\mathrm{Tb}}_{h_{11/2^-}} - 3E^{^{145}\mathrm{Eu}}_{d^{-1}_{5/2^+}} - 3E^{^{145}\mathrm{Eu}}_{g^{-1}_{7/2^+}} - 6E^{^{147}\mathrm{Gd}}_{f_{7/2^-}} + S_{\pi^{+1}\pi^{-2}\nu^2}\\
&\quad = 5057_{92}\ \text{keV},
\end{aligned}
$$

where

$$
\begin{aligned}
S_{\pi^{+1}\pi^{-2}\nu^2} &= -M^{^{147}\mathrm{Eu}} + 8M^{^{146}\mathrm{Gd}} + M^{^{144}\mathrm{Sm}} + M^{^{148}\mathrm{Gd}} + 2M^{^{148}\mathrm{Tb}}\\
&\quad + 4M^{^{146}\mathrm{Eu}} - 3M^{^{147}\mathrm{Tb}} - 6M^{^{146}\mathrm{Eu}} - 6M^{^{147}\mathrm{Gd}}\\
&= -6513_{92}\ \text{keV}.
\end{aligned}
$$

Shell model diagonalizations give the energies of the configuration's remaining 1134 levels, but in Fig. 6 we show only the configuration yrast states for the higher spins where the $\pi^{-2}_{0^+}$ and $(\pi h_{11/2}d^{-1}_{5/2})_{3^-}$ couplings essentially do not contribute to the energy. Corresponding results for the $(\pi h_{11/2}d^{-2}_{5/2}\nu f^2_{7/2})$ and $(\pi h_{11/2}g^{-2}_{7/2}\nu f^2_{7/2})$ five-nucleon configurations are also shown.

Our experiment could not conclusively identify the fully aligned $35/2^-$ state, but theory agrees well with the firmly characterized $31/2^-$ level at 4284 keV. Its decay through a 1384 keV $E2$ γ ray is not configuration specific, but for the ^{147}Eu five-quasiparticle levels such high energy interconfiguration γ decay often dominates over low energy $M1$ deexcitation within the configuration. Above this $31/2^-$ state the data cannot specify any clearcut odd-parity levels; however, we note that the 4639 keV 33/2 state lies close to the shell model prediction, and its 845 keV ($E1$) decay is not in conflict with this assignment. An even more speculative candidate for the aligned state is the 35/2 level at 4862 keV, with, however, exclusive 250 keV ($E1$) interconfiguration decay, much in contrast to expectation. Moreover the level parity again is unknown and nearby 35/2 states abound. We also note the good agreement of the calculated $23/2^-$ energy with the complex 2845 keV $23/2^-$ octupole state discussed above, which does not elucidate the situation further.

Finally, we mention that attempts to calculate in a similar way the even-parity five-quasiparticle excitations proved completely unsuccessful. Contrary to ^{149}Tb these levels now include the $\pi^{-2}_{0^+}$ two-proton-hole 0^+ pair boson and consequently all input data must include that boson as well. The inherent principle of the shell model reduction requires that this boson remains strictly unaffected in all combinations with the different one- and two-fermion partners. This might only approximately be fulfilled and thus could be one cause for the failure of our calculation for these levels.

VI. CONCLUSIONS

In a ^{124}Sn(^{28}Si,$p4n$) experiment with a detection sensitivity of 1% of the exit channel we have significantly extended the high spin level scheme of the two-neutron one-proton-hole nucleus ^{147}Eu. Up to the highest levels close to 10 MeV and $I\sim 55/2$ the results clearly reveal the characteristic features of multiparticle configurations in a spherical nucleus, and specific configurations are proposed for almost all states. We find that the observed ^{147}Eu levels up to 6 MeV have clear counterparts in the isotone ^{149}Tb at very similar energies relative to the respective $\pi h_{11/2}$ isomers. The excitations up to 4.2 MeV are classified as three-nucleon configurations and their couplings to the ^{146}Gd core octupole phonon. We obtain excellent quantitative agreement with experiment of the results of parameter-free shell model calculations where both the fermion-fermion and fermion-boson two-body interactions are taken from experiment, and where the coupling to the two-proton-hole 0^+ boson is explicitly calculated.

ACKNOWLEDGMENTS

The authors acknowledge the staff of the XTU Tandem of LNL for the stable operation of the accelerator. They also wish to thank R. Julin for valuable information on his (p,n) data, and P. Wieder (FZ. Jülich) for valuable help. This work was partially supported by the E.C. under Contract No. ERBFMGECT980110. One of us (P.K.) acknowledges support of the Ministerio de Educacion y Ciencia, Spain and C.S.I.C, Spain. A.G. was supported by the E.C. under Contract No. ERBFMBICT983127.

[1] M. Piiparinen, P. Kleinheinz, S. Lunardi, M. Ogawa, G. de Angelis, F. Soramel, W. Meczynski, and J. Blomqvist, Z. Phys. A **337**, 387 (1990).
[2] M. Lach, P. Kleinheinz, M. Piiparinen, M. Ogawa, S. Lunardi, M. C. Bosca, J. Styczen, and J. Blomqvist, Z. Phys. A **341**, 25 (1991).
[3] E. der Mateosian and L. K. Peker, Nucl. Data Sheets **66**, 705 (1992).
[4] E. P. Grigorev, A. V. Zolotavin, S. V. Kamynov, V. O. Sergeev, T. Vylov, and V. G. Kalinnikov, Izv. Akad. Nauk SSSR, Ser. Fiz. **41**, 1203 (1977).
[5] L. G. Mann, D. J. Decman, H. E. Martz, T. N. Massey, G. L. Struble, P. Kleinheinz, H. J. Scheerer, D. G. Burke, and G. Kajrys, Z. Phys. A **337**, 301 (1990).
[6] G. Lo Bianco, N. Molho, A. Moroni, A. Bracco, and N. Blasi, J. Phys. G **7**, 219 (1981).
[7] R. Julin, A. Pakkanen, M. Piiparinen, B. Rubio, and P. Kleinheinz, JFYL Annual Report 1984–1985, 1985, p. 63.
[8] J. G. Fleissner, E. G. Funk, F. P. Venezia, and W. Mihelich, Phys. Rev. C **16**, 227 (1977).
[9] X. H. Zhou, E. Ideguchi, Y. Gono, T. Kishida, S. Mitarai, T. Morikawa, H. Tsuchida, M. Shibata, H. Watanabe, M. Miyake, A. Odahara, M. Oshima, Y. Hatsukawa, S. Hamada, H. Iimura, M. Shibata, T. Ishii, and M. Ishihara, Z. Phys. A **358**, 285 (1997).
[10] D. S. Haslip, N. Kintz, S. Flibotte, R. A. E. Austin, G. de France, M. Devlin, Ch. Finck, A. Galindo-Uribarri, G. Gervais, D. R. LaFosse, T. J. Lampman, I. Y. Lee, F. Lerma, A. O. Macchiavelli, R. W. MacLeod, S. M. Mullins, J. N. Nieminen, T. Rodinger, D. G. Sarantites, O. Stezowski, C. E. Svensson, J. P. Vivien, J. C. Waddington, D. Ward, and J. N. Wilson, Phys. Rev. C **57**, 2196 (1998).
[11] D. Bazzacco, Proceedings of the International Conference on Nuclear Structure at High Angular Momentum, Ottawa, 1992, Vol. 2 of Proceedings AECL 10613, p. 376.
[12] Z. Méliani, J. S. Dionisio, C. Schück, Ch. Vieu, F. A. Beck, T. Byrski, D. Curien, G. Duchêne, J. C. Merdinger, P. Fallon, J. W. Roberts, and J. F. Sharpey-Schafer, Nucl. Phys. **A575**, 221 (1994).
[13] A. Ercan, R. Broda, M. Piiparinen, Y. Nagai, R. Pengo, and P. Kleinheinz, Z. Phys. A **295**, 197 (1980); A. Ercan *et al.*, in *Proceedings of the International Conference on Nuclear Physics*, Florence, 1983, edited by E. Blasi and R. A. Ricci (Tipografia Compositori, Bologna, 1984), Vol. 1, p. 154.
[14] T. I. Kracikova, M. Finger, S. Davaa, V. M. Tsupko-Sitnikov, V. A. Deryuga, and W. D. Hamilton, Nucl. Phys. **A408**, 45 (1983).
[15] C. T. Zhang, P. Kleinheinz, M. Piiparinen, R. Broda, R. Collatz, P. J. Daly, K. H. Maier, R. Menegazzo, G. Sletten, J. Styczen, and J. Blomqvist, Phys. Rev. C **54**, R1 (1996).
[16] R. Collatz, P. Kleinheinz, R. Menegazzo, R. Broda, C. T. Zhang, J. Blomqvist, J. Rico, and A. Gadea, KFA-IKP Annual Report 1990, 1991, p. 25.
[17] J. Styczen, P. Kleinheinz, W. Starzecki, B. Rubio, G. de Angelis, H. J. Hähn, C. F. Liang, P. Paris, R. Reinhardt, P. von Brentano, and J. Blomqvist, in Nuclei Far from Stability, Rosseau Lake, 1987, edited by Ian S. Towner, AIP Conf. Proc. No. 164 (AIP, New York, 1988), p. 489; Institut für Kernphysik, KFA-Jülich, Annual Report, 1987, p. 47.
[18] G. de Angelis, P. Kleinheinz, B. Rubio, J. L. Tain, K. Zuber, B. Brinkmoller, P. von Rossen, J. Romer, D. Paul, J. Meissburger, G. P. A. Berg, A. Magiera, G. Hlawatsch, L. G. Mann, T. N. Massey, D. Decman, G. L. Struble, and J. Blomqvist, Z. Phys. A **336**, 375 (1990).
[19] B. Rubio, P. Kleinheinz, A. Ercan, R. Julin, L. G. Mann, W. Stöff, E. A. Henry, V. Dave, and J. Blomqvist, Proceedings of XX Winter School, Zakopane, Poland, 1985, p. 369; B. Rubio, P. Kleinheinz, A. Ercan, R. Julin, M. Lach, L. G. Mann, W. Stöffl, E. A. Henry, V. Dave, and J. Blomqvist, Proceedings of the International Nuclear Physics Conference, Harrogate, 1986, Vol. 1, p. 165.
[20] R. Broda, M. Behar, P. Kleinheinz, P. J. Daly, and J. Blomqvist, Z. Phys. A **293**, 135 (1979).
[21] G. Audi, O. Bersillon, J. Blachot, and A. H. Wapstra, Nucl. Phys. **A624**, 1 (1997).
[22] J. Rico, B. Rubio, J. L. Tain, A. Gadea, J. Bea, L. M. Garcia-Raffi, O. Tengblad, P. Kleinheinz, R. Menegazzo, R. Wirowski, P. von Brentano, G. Siems, and J. Blomqvist, Z. Phys. A **345**, 245 (1993).
[23] R. Menegazzo, P. Kleinheinz, R. Collatz, H. Guven, J. Styczen, D. Schardt, H. Keller, O. Klepper, G. Walter, A. Huck, G. Marguier, J. Blomqvist, and the ISOLDE Collaboration, Z. Phys. A **349**, 13 (1994).
[24] H. Kader, G. Graw, F. J. Eckle, G. Eckle, P. Schiemenz, P. Kleinheinz, B. Rubio, G. de Angelis, T. N. Massey, L. G. Mann, and J. Blomqvist, Phys. Lett. B **227**, 325 (1989).
[25] L. M. Garcia-Raffi, B. Rubio, J. L. Tain, J. Bea, A. Gadea, J. Rico, P. Kleinheinz, R. Menegazzo, R. Wirowski, P. von Brentano, G. Siems, and A. Dewald, Z. Phys. A **358**, 205 (1997).
[26] B. Rubio *et al.*, IKP KFA Jülich Annual Report 1985 (unpublished), p. 35; [19].
[27] A. Ercan, R. Broda, P. Kleinheinz, M. Piiparinen, R. Julin, and J. Blomqvist, Z. Phys. A **329**, 63 (1988).
[28] P. Kleinheinz, M. Ogawa, R. Broda, P. J. Daly, D. Haenni, H. Beuscher, and A. Kleinrahm, Z. Phys A **286**, 27 (1978).
[29] S. W. Yates, R. Julin, P. Kleinheinz, B. Rubio, L. G. Mann, E. A. Henry, W. Stoffl, D. J. Decman, and J. Blomqvist, Z. Phys. A **324**, 417 (1986).